
The mechanism of silver deposition and dissolution in cyanide electrolytes

Gintaras Baltrūnas and
Edita Pakalnienė

Department of Physical Chemistry,
Vilnius University,
Naugarduko 24,
LT-2006, Lithuania

To study the mechanism of the electrochemical reaction: $\text{Ag}(\text{CN})_x^{1-x} + e^- \rightleftharpoons \text{Ag} + x\text{CN}^-$, the FFT impedance spectra were measured in the frequency range from 0.03 to 950 Hz at a constant silver cyanide complex concentration (0.05 M) and different free cyanide ion concentrations (from 0.01 to 1.0 M). The analysis of the impedance spectra was carried out taking into account the cyanide adsorption/desorption process and the variation of the active surface area of electrode surface with the cyanide concentration. The exchange current density re-calculated for only the active area gives the electrochemical reaction order ($R_{\text{CN}} = 1.8$ for $\alpha = 0.5$, and $R_{\text{CN}} = 2$ for $\alpha = 0.6$) which is independent of CN^- concentration and of the composition of the complexes prevailing in the bulk of the electrolyte. The value of R_{CN} close to 2, obtained in a series of isopotential solutions ($E_0 = -0.350$ V) confirms that in all cases the complex ions $\text{Ag}(\text{CN})_2^-$ take a direct part in the charge transfer step.

Key words: silver, cyanide, partially blocked electrodes, mechanism

INTRODUCTION

The first study of the mechanism of the electrochemical reaction: $\text{Ag}(\text{CN})_x^{1-x} + e^- \rightleftharpoons \text{Ag} + x\text{CN}^-$ in solutions containing various amounts of KCN was carried out by the chronoamperometric method [1]. The analysis of the data has led to the conclusion that in the concentration range $[\text{CN}^-] < 0.1$ M, the complex particle directly involved in the charge transfer is AgCN , whereas at higher concentrations $[\text{CN}^-] > 0.2$ M, the electrochemical reaction occurs via a different mechanism, where the charge transfer step involves the $\text{Ag}(\text{CN})_2^-$ particle. This mechanism was partially confirmed in Ref. [2, 3]. Analysis of the kinetic parameters of the reaction has led to the conclusion that at a higher cyanide concentration ($[\text{CN}^-] > 0.2$ M) the reaction order $R_{\text{CN}} = 1.88$ [2]. The authors in ref. [3] used the method of isopotential solutions and the rotating disc electrode technique to investigate this reaction. They found R_{CN} values to be in the interval from 1.04 to 1.21, at cyanide concentrations from 0.01 to 0.25 M. To confirm the mechanism of the electrochemical reaction proposed in [1], new chronoamperometric measurements have been carried out using an improved measurement technique [4]. The reaction order R_{CN} was found to be within a narrow interval from approximately 1.2 to 1.4. In this work, the authors suggested that the reaction rate might be af-

→
←
fected by the adsorption of cyanide ions. In addition, at a certain reaction step, the partial charge transfer could occur. The analysis of the electrochemical impedance data [5] has brought the interpretation of the results back to the scheme initially proposed in Ref. [1]. In addition, the scheme was extended for the cyanide concentration range above 0.9 M. It was suggested that in this concentration range the charge transfer process involves the complex particle $\text{Ag}(\text{CN})_3^-$.

The measurements of the surface stress revealed a significant influence of the cyanide adsorption on the properties of the electrodeposited silver layer [6]. It has been found that the cyanides adsorb irreversibly on the silver surface during electrodeposition. This irreversible adsorption causes passivation of the surface, which changes appreciably the peculiarities of the reduction of the silver complexes, which are reflected by the changed voltammetric, chronoamperometric and electrochemical impedance behavior [7]. Measuring the amount of the electrodeposited silver by the quartz microbalance technique under potentiostatic conditions, the authors of Ref. [8] have found discrepancies between the charge consumed and the mass change during the initial moment (< 3 s) of electrodeposition. This suggested the conclusion that in parallel to the reduction of the silver complexes, the cyanide ion oxidation could occur. The possible product of the oxidation might

be the two-dimensional surface compound paracyanogen $(\text{CN})_{2n}$. The degree of the surface blockage is highly sensitive to the cyanide concentration. For example, when $[\text{CN}^-] \leq 0.01 \text{ M}$, almost the whole surface of the silver electrode is active. However, at $[\text{CN}^-] \geq 0.5 \text{ M}$ only about 20% of the surface remains active [9]. The exchange current density (j_0) of the electrochemical reaction is much lower on the passive sites of the surface than that on the active ones [10]. Thus the surface blockage degree θ could be a function of cyanide concentration. This fact was not taken into account by earlier investigators [1–5]. Therefore, the reaction order R_{CN} obtained by the earlier authors could be noticeably distorted. In the present work, we have attempted to establish the mechanism of the electrochemical reaction, taking into account the possible variation of the active surface area.

The analysis of the impedance spectra for partially blocked electrodes in the case of semi-infinite diffusion was carried out by Matsuda et al. [11]. Later Lorentz et al. [12, 13] and Gabrielli et al. [14] extended the theory for the case of the finite diffusion layer thickness. Except the surface patches covered by irreversibly adsorbed cyanide ions, the remaining surface area is involved in the reversible cyanide adsorption/desorption process. At relatively high frequencies, the impedance spectra could be modeled by the equivalent scheme that consists of uncompensated electrolyte resistance, double-layer capacitance, charge transfer resistance, diffusion impedance and cyanide adsorption/desorption capacitance and resistance [15]. We have used a polycrystalline silver electrode whose surface was definitely rough. In general, the constant phase element (*CPE*) should be used instead of the double layer capacitance (C_D). The impedance of the (*CPE*) could be expressed as $Z_{\text{CPE}} = A^{-1}(j\omega)^{-n}$, where A is the *CPE* constant, n is the *CPE* exponent that reflects the deviation of the impedance phase from -90 degrees and ω is the cyclic frequency. In the investigated system the *CPE* exponent values exceeded 0.94. Therefore, we assumed the approximation $Z_{\text{CPE}} = A^{-1}(j\omega C_D)^{-1}$ and used the capacitor instead of *CPE* throughout the work. In accordance to this equivalent circuit, the deviations of the impedance spectra from experimental data did not exceed 2.5%. The deviations were randomly distributed along the theoretical curve.

The double-layer capacitance calculated in accordance to the above scheme corresponds to the sum of the double-layer capacitances on the active and blocked sites. The remaining parameters correspond only to the active sites. In other words, they reflect simultaneously both the electrochemical parameter and the surface blocking degree.

EXPERIMENTAL

The experiments were carried out under the nitrogen atmosphere at 20°C . The conventional three-electrode cell was used throughout the work. The working electrode was a silver disc pressed into flouroplast with the 0.35 cm^2 surface area exposed to the solution. Before each measurement the surface was cleaned mechanically and degreased. In this work, all potentials are referred to the scale of the standard hydrogen electrode. The solutions were prepared using twice-distilled water. The salts KCN, KF, NaOH and $\text{KAg}(\text{CN})_2$ were chemically pure (Merck). All measurements were started exactly 100 s following the immersion of the working electrode into solution. The choice of the immersion moment was based upon blocking dynamics established previously in Ref. [15].

The EIS measurements were performed either potentiostatically at the equilibrium potential or galvanostatically at zero current, using a fast Fourier transform (FFT) impedance spectrometer connected to the cell via a fast potentiostat/galvanostat as described in more detail elsewhere [16, 17]. The peak-to-peak amplitude of the perturbation voltage was 10 mV. For measurements in the galvanostatic regime, the amplitude of the perturbation current was chosen in such a way that the response voltage would not exceed 10–15 mV. The impedance spectra obtained were validated by comparing the power spectra of perturbation and response as described in [18]. Time-resolved EIS measurements were performed as a series of 16 spectra. The LEVM software by J. R. Macdonald [19] was used for the analysis of the impedance spectra.

RESULTS AND DISCUSSION

Full electrochemical impedance spectra in the range of 0.03 to 950 Hz were recorded in the solutions containing 0.05 M $\text{KAg}(\text{CN})_2$ and 0.01 to 1.0 M KCN. In order to maintain similar conductivity and ionic strength of the working solutions we kept the sum of the concentrations $\text{KCN} + \text{KF} = 1 \text{ M}$. We have chosen KF as an indifferent electrolyte, because it has almost no influence on the impedance spectra in this system [15].

In the ultra-low (0.03–0.16 Hz) frequency range, the dependencies of the real component of impedance ($\text{Re } Z$) on cyclic AC current frequency (ω) are linear in the coordinates $\text{Re } Z - \omega^{-1/2}$ (Fig. 1). Thus, according to [11] the Warburg constant (W_0) could be established easily:

$$\left(\frac{\partial \text{Re } Z}{\partial \omega^{-1/2}} \right)_{\omega \rightarrow 0} = W_0. \quad (1)$$

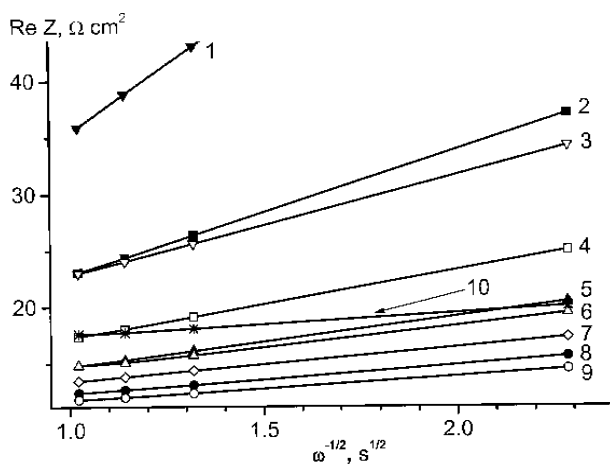


Fig. 1. Frequency dependence of the real component of silver electrode. Solution: $KAg(CN)_2 - 0.05\text{ M}$, $NaOH$ – up to pH 13, $KCN + KF = 1\text{ M}$, $KCN\text{ (M)}$: 1 – 0.01, 2 – 0.02, 3 – 0.03, 4 – 0.057, 5 – 0.092, 6 – 0.13, 7 – 0.2, 8 – 0.33, 9 – 0.5, 10 – 1.0

The dependence of this constant on the concentration of free $[CN^-]$ ions is shown in Fig. 2 (curve 1). When the concentration of cyanide is changed from 0.01 to 1 M, the Warburg constant decreases from 24 to $1.9\ \Omega\text{ cm}^2\text{ s}^{1/2}$. At higher cyanide concentrations, the contribution of migration to the overall mass transport process might become noticeable. Because of this contribution one could expect a slight increase in W_0 values. However, this deviation will equally affect both W_0 and $W_0 / (1-\theta)$. In our investigation, only the ratio of these two quantities is important. Thus, the possible contribution of the migration cannot affect the calculation results.

For the further analysis, in accordance to the equivalent circuit shown in Fig. 3 we used a relatively high ($f > 10\text{ Hz}$) frequency range (Fig. 4). It seemed that the frequency interval (10–950 Hz) used to establish six parameters ($R_0, C_D, R_{ct}, W_0 / (1-\theta)$,

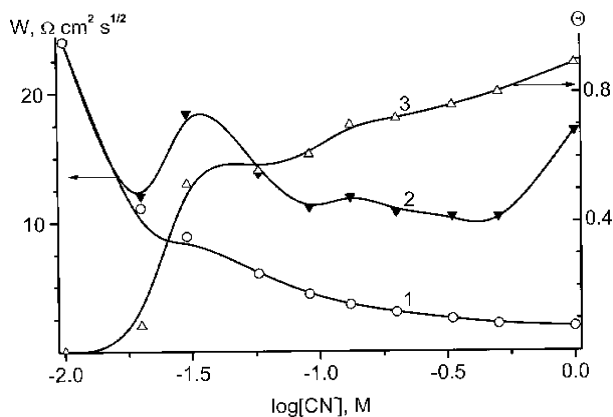


Fig. 2. Dependences of W_0 (1), $W_0/(1-\theta)$ (2) and θ (3) on cyanide concentration

R_A, C_A) was too small. In order to verify this, we recorded several more spectra in the interval of 10–12500 Hz. However, the obtained result was the same. This might be due to the favorable distribution of the parameters. Conversely, the attempt to decrease the number of fitting parameters was not successful. For example, it was impossible to describe the spectrum if R_A and C_A were expelled from the fitting parameter set. At the same time, the chi-squared function increased from 0.00049 to 0.014. It is enough to increase R_A two-fold to alter the values of the other parameters, e.g., $1.2 R_0, 1.3 C_D, 0.79 R_{ct}, 0.49 C_A$, etc. Simultaneously, the error of the fit parameters noticeably increases. For example, the error of C_A increases to 31%, while normally the errors of all parameters do not exceed 3%. In addition, the overall spectra-fit quality decreases, what is reflected in the chi-squared function change from 0.00049 to 0.0031. Given the results of the present analysis, one might expect that the established parameter values are sufficiently reliable.

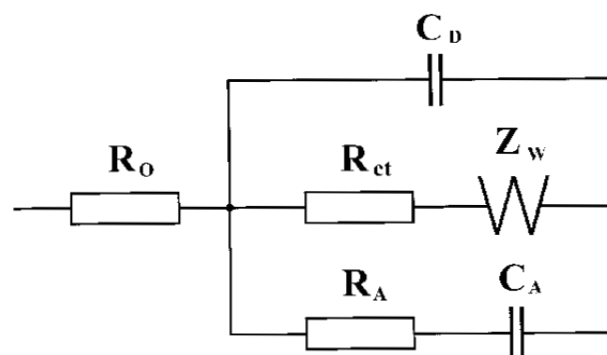


Fig. 3. Electrical equivalent circuit. R_A and C_A are resistance and capacitance which account for the adsorption/desorption processes. R_{ct} and C_D are the charge transfer resistance and the double layer capacitance, R_0 represents the uncompensated electrolyte resistance, and Z_w is the Warburg impedance

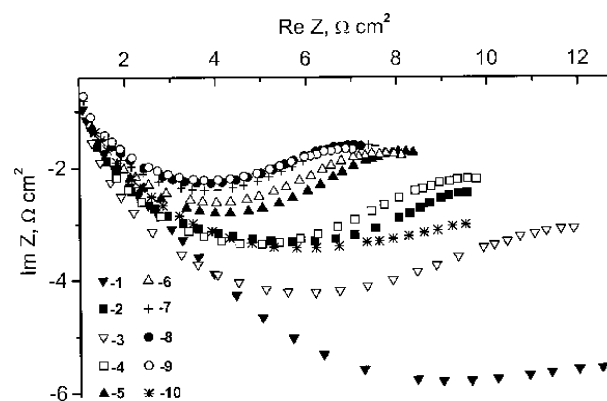


Fig. 4. Impedance spectra of silver electrode (10–950 Hz). Solution composition as in Fig. 1

The obtained $W_0 / (1-\theta)$ values are presented in Fig. 2 (curve 2). The electrolyte ohmic resistance was varying negligibly in the investigated solutions. Its value was within the interval 0.85 to 0.95 $\Omega \text{ cm}^2$. The other parameters of the equivalent circuit depended noticeably upon cyanide concentration. The double-layer capacitance (90–160 $\mu\text{F cm}^{-2}$) and the cyanide adsorption capacitance (35–135 $\mu\text{F cm}^{-2}$) pass through a shallow minimum at a $[\text{CN}^-]$ concentration of about 0.1 M. On the contrary, the dependence of cyanide adsorption resistance (11–34 $\Omega \text{ cm}^2$) on the cyanide bulk concentration exhibits a sharp maximum. For the present investigation, the most important parameters R_{ct} (Fig. 5, curve 1) and $W_0 / (1-\theta)$ (Fig. 2, curve 2) vary in a complex way, though they have some similar features. From W_0 and $W_0 / (1-\theta)$ values presented in Fig. 2, the dependence of the silver electrode blockage degree on the free cyanide concentration (Fig. 2, curve 3) has been calculated. The obtained dependency is similar to that described by us earlier [9].

According to [20], for the dependence of exchange current density on free cyanide concentration, the following equation is valid:

$$\log j_0 = \text{const} + R_{CN} \log[\text{CN}^-] + \frac{zF\alpha}{2.303RT} E_0. \quad (2)$$

Under assumption that $z = 1$ and $\alpha = 0.5$ [1], this expression could be rewritten as

$$\log j_0 = \text{const} + R_{CN} \log[\text{CN}^-] + 8.684E_0. \quad (3)$$

The constant could be established from the $\log j_0$ value at $[\text{CN}^-] = 0.01 \text{ M}$, because in this case all the surface of the electrode is active. Then ($E_0 = -0.254 \text{ V}$, $j_0 = 2.31 \text{ mA cm}^{-2}$):

$$\text{const} = 2R_{CN} + 2.27. \quad (4)$$

As follows from Eq. 2, in order to establish the reaction degree one should precisely know the dependence of the equilibrium potential of the electrode on the free cyanide concentration. In the region of low $[\text{CN}^-]$ concentrations, the complex $\text{Ag}(\text{CN})_2$ dominates in the solution. However, when the concentration of $[\text{CN}^-]$ is increased, the complex $\text{Ag}(\text{CN})_3^{2-}$ becomes dominant in the system. That is the reason why the quantity $\partial E_0 / \partial \ln[\text{CN}^-]$ varies with the cyanide concentration. The influence of this variation could be estimated, if the equilibrium constant for the reaction $\text{Ag}(\text{CN})_2^- + \text{CN}^- \rightleftharpoons \text{Ag}(\text{CN})_3^{2-}$ is known. However, different authors provide different values of this constant. In addition, this value could be sensi-

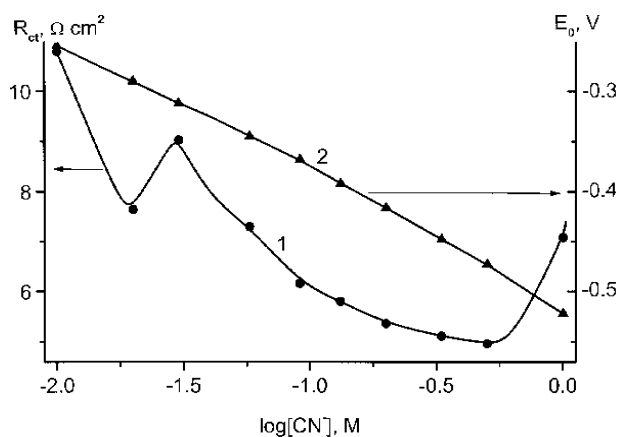


Fig. 5. Dependences of charge transfer resistance (1) and silver electrode equilibrium potential (2) on cyanide concentration

tive to the ionic strength. That is why we have performed independent measurements of the reversible silver electrode potential. The results are plotted in Fig. 5 (curve 2).

Equation (3) was used to calculate the dependences of the exchange current density on the cyanide concentration at various values of R_{CN} (solid curves in Fig. 6). In Fig. 6 we also present $j_0 / (1-\theta)$ (open circles) and j_0 (solid circles) dependences, which were obtained from the charge transfer resistance and surface blockage degree:

$$\frac{j_0}{1-\theta} = \frac{RT}{zFR_{ct}}. \quad (5)$$

As is seen from the data presented in Fig. 6, if one does not take into account the surface blockage (open circles), the $\log j_0$ dependence on cyanide concentration is negligible as was reported in [4]. The R_{CN} calculated from this plot would be equal to 1.3. However, if one takes into account the variation of the active surface area with cyanide concentration, the $\log j_0$ dependence from the $[\text{CN}^-]$ concentration becomes more pronounced (solid circles). Correspondingly, the calculated reaction order increases approximately to 2. The best fit using eq. 3 was observed at $R_{CN} = 1.8$.

Several reasons could be responsible for the inconsistency between the experimental value $R_{CN} = 1.8$ and the theoretical value 2. First, the surface blockage degree was estimated from the diffusion impedance measurements, which are sensitive only to the presence of relatively large (in our case larger than 5 μm) passive regions on the surface. Therefore, it is possible that the real surface blockage degree could be higher than follows from Fig. 2. In this case, the calculation of the exchange current to the active surface area yields lower $\log j_0$ values.

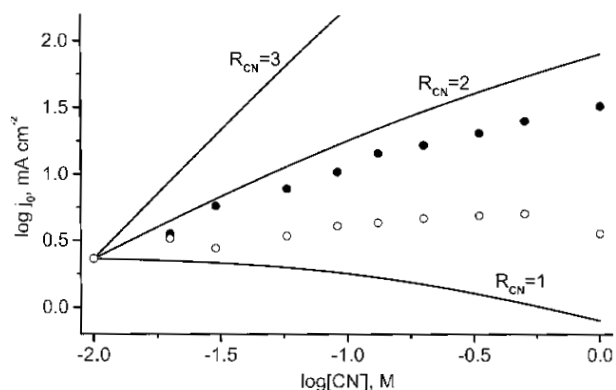


Fig. 6. Dependences of exchange current density on cyanide concentration. Solid curves are calculated via Eq. (3) at different R_{CN} values. Circles show the experimentally determined exchange current values: open circles show the values calculated with respect to all electrode surface area, solid circles show the values calculated with respect to the active surface area

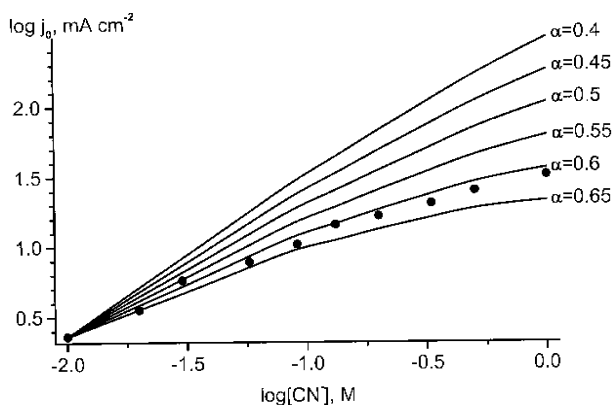


Fig. 7. Dependences of exchange current density on cyanide concentration. Solid curves are calculated via Eq. (3) for $R_{CN} = 2$ and different α values. Circles show the experimentally determined exchange current values calculated with respect to the active surface area

However, the estimation of the possible errors performed on the basis of Eqs. (8) and (11) shows that a 10% relative error of θ yields approximately a 5% error in the value of R_{CN} . Second, the theoretical $\log j_0 - \log [CN^-]$ dependences are influenced by the α value of parameter, while in several works [1–4] the values of this coefficient were found to be slightly different. In order to find the α value that describes most precisely the relationship between experimental $\log j_0$ and $\log [CN^-]$, we modeled this relationship using Eq. (2). As an initial condition, the quantities $z = 1$ and $R_{CN} = 2$ were fixed. From Fig. 7 it is clear that the best fit could be obtained when $0.6 < \alpha < 0.65$. It is interesting to note that for the solution of similar composition very close α values were reported in Ref. [4]. For this reason,

one might conclude that in the concentration interval $0.01 < [CN^-] < 1$ M $R_{CN} = 2$, i.e., the particle $Ag(CN)_2^-$ is directly involved in the charge transfer stage.

There is another possibility to evaluate the reaction order in the case when the value of the charge transfer coefficient α is not known precisely. It is the isopotential solution series method [3]. The potential of silver electrode depends both on the free cyanide concentration and the concentration of the complexes. Therefore, in a certain $[CN^-]$ concentration range, one may choose the appropriate $Ag(CN)^{1-x}_x$ concentrations, which would yield the same E_0 value. For such series of isopotential solutions ($E_0 = const$), the differentiation of Eq. (2) leads to

$$\left(\frac{\partial \log j_0}{\partial \log [CN^-]} \right)_{E_0} = R_{CN} \quad (6)$$

It is clear that for the series of isopotential solutions the plot $\log j_0$ vs. $\log [CN^-]$ is a line with the slope R_{CN} . So, R_{CN} could be evaluated without knowing the charge transfer coefficient α . We used the solutions containing CN^- ions from 0.03 to 0.15 M (Table), which yielded the potential of the silver electrode $E_0 = -0.350$ V. The formation of $Ag(CN)_3^{2-}$ was taken into account during preparation of the solutions, because some portion of the cyanide ions is consumed in the reaction: $Ag(CN)_2^- + CN^- \rightleftharpoons Ag(CN)_3^{2-}$. The equilibrium constant ($K_C = 8$) of the latter reaction was estimated from the dependence of E_0 on $[CN^-]$ (Fig. 5, curve 2). As described above, the impedance spectra of the Ag electrode were taken in these solutions. The W_0 values were estimated from the low-frequency portion of the im-

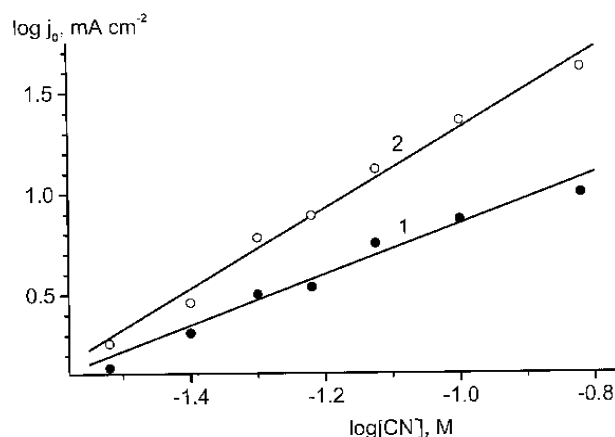


Fig. 8. Dependences of the exchange current density on the cyanide concentration in isopotential solutions (Table): 1 – calculated with respect to all electrode surface area; 2 – calculated with respect to the active surface area

Table. Parameters of electrochemical system determined by the impedance method in isopotential solutions

Isopotential solution			Electrochemical system parameters				
KAg(CN) ₂ M	KCN M	[CN ⁻] ¹ M	W ₀ Ω cm ² s ^{1/2}	W ₀ / (1-θ) Ω cm ² s ^{1/2}	θ	C _D μF cm ⁻²	R _α Ω cm ²
0.015	0.034	0.031	12.7	16.7	0.24	89.1	18.1
0.0235	0.047	0.041	9.33	13.14	0.29	86.4	12.2
0.035	0.067	0.052	7.27	13.85	0.48	85.2	7.91
0.048	0.078	0.061	6.01	13.66	0.56	85.3	7.29
0.069	0.105	0.075	4.84	11.36	0.57	88.7	4.45
0.118	0.159	0.101	3.63	11.2	0.68	93.8	3.37
0.27	0.312	0.152	2.45	10.21	0.76	99.7	2.5

¹ Free ions.

pedance spectrum. The high-frequency portion of the impedance spectrum was analyzed in accordance to the equivalent circuit shown in Fig. 3, and all elements were obtained by a fitting procedure. The values of the main equivalent circuit elements are presented in Table. In the way already described above, the dependences $\log j_0$ vs. $\log [CN^-]$ were calculated both ignoring (Fig. 8, curve 1) and taking into account (Fig. 8, curve 2) a possible surface blockage of the silver electrode. As is seen from the data, in both cases one observes practically linear dependences, however, having different slopes. If one ignores the surface blockage process, $R_{CN} = 1.21$, *i.e.*, rather close to the value calculated in Ref. [3]. However, if one takes into account the surface blockage and its dependence on the $[CN^-]$ concentration, $R_{CN} = 2.02$, what confirms the earlier presented results with $\alpha \approx 0.6$.

CONCLUSIONS

The FFT analysis of the impedance spectra was carried out taking into account the cyanide adsorption/desorption process and the variation of the active surface area of the electrode with the cyanide concentration. These results show that independently of the free cyanide concentration and the composition of the complex ion that dominates in the bulk of the solution, the particle involved in the charge transfer step is $Ag(CN)_2^-$ ion. At a higher cyanide concentration in the bulk, the complex particle $Ag(CN)_3^{2-}$ dominates in the solution. In this case, the fast chemical reaction $Ag(CN)_3^{2-} \rightleftharpoons Ag(CN)_2^- + CN^-$ should occur near the surface prior to the charge transfer: $Ag(CN)_2^- + e^- \rightleftharpoons Ag + 2CN^-$.

Received 18 January 2002
Accepted 1 February 2002

References

1. W. Vielstich and H. Gerischer, *Z. Phys. Chem. NF*, **4**, 10 (1955).
2. E. A. Nechaev and R. Y. Bek, *Sov. Electrochem.*, **2**, 138 (1966).
3. A. A. Survila, E. I. Morkiavicius, and A. A. Dikcius, *Sov. Electrochem.*, **21**, 1351 (1985).
4. H. Baltruschat and W. Vielstich, *J. Electroanal. Chem.*, **154**, 141 (1983).
5. O. A. Ashiru and J. P. G. Farr, *J. Electrochem. Soc.*, **142**, 3729 (1995).
6. G. Valincius, *Sov. Electrochem.*, **28**, 654 (1992).
7. G. Baltrunas, V. Drunga, and D. Svedas, *J. Electroanal. Chem.*, **369**, 93 (1994).
8. V. Daujotis, D. Jasaitis, and R. Raudonis, *Electrochim. Acta.*, **42**, 1337 (1997).
9. G. Baltrunas and V. Drunga, *Sov. Electrochem.*, **28**, 889 (1992).
10. G. Baltrunas, E. Morkevicius, and A. Dikcius, *Sov. Electrochem.*, **26**, 791 (1990).
11. T. Gueshi, K. Tokuda, and H. Matsuda, *J. Electroanal. Chem.*, **102**, 41 (1979).
12. J. Hitzig, J. Titz, K. Juttner, W. J. Lorenz, and E. Schmidt, *Electrochim. Acta.*, **29**, 287 (1984).
13. E. Schmidt, J. Hitzig, J. Titz, K. Juttner, and W. J. Lorenz, *Electrochim. Acta.*, **31**, 1041 (1986).
14. C. Deslouis, C. Gabrielli, M. Keddou, A. Khalil, R. Rasset, B. Tribollet, and M. Zidoune, *Electrochim. Acta.*, **42**, 1219 (1997).
15. G. Baltrunas, G. S. Popkirov, and R. N. Schindler, *J. Electroanal. Chem.*, **435**, 95 (1997).
16. G. S. Popkirov and R. N. Schindler, *Rev. Sci. Instrum.*, **63**, 5366 (1992).
17. G. S. Popkirov and R. N. Schindler, *Rev. Sci. Instrum.*, **64**, 3111 (1993).
18. G. S. Popkirov and R. N. Schindler, *Electrochim. Acta.*, **38**, 861 (1993).
19. J. R. Macdonald, *CNLS/LEVM program*, can be obtained by Solartron Ltd.
20. K. J. Vetter, *Electrochemical Kinetics*, Academic Press, New York, 1967.

G. Baltrūnas, E. Pakalniė

**SIDABRO TIRPIMO IR NUSODINIMO
CIANIDINIUOSE ELEKTROLITUOSE
MECHANIZMAS**

S a n t r a u k a

Elektrocheminės reakcijos $\text{Ag}(\text{CN})_x^{1-x} + e^- \rightleftharpoons \text{Ag} + x\text{CN}^-$ mechanizmui tirti buvo nustatyti FFT pilnutinės varžos spektrai 0,0305 ÷ 946 Hz srityje, esant pastoviai (0,05 M) sidabro cianidinių kompleksų ir skirtingoms (0,01 ÷ 1,0 M)

laisvų cianido jonų koncentracijoms. Analizuojant spektrus buvo atsižvelgiama į cianidų adsorbcijos–desorbcijos procesą bei elektrodo paviršiaus aktyvaus ploto priklausomybę nuo cianidų koncentracijos. Perskaičiavus mainų srovės tankį tik į aktyvųjį plotą, nustatytas elektrocheminės reakcijos laipsnis pagal cianidus ($R_{\text{CN}} = 1,8$, kai $a = 0,5$ ir $R_{\text{CN}} = 2$, kai $a = 0,6$), kuris nepriklauso nuo CN^- koncentracijos bei tirpalo tūryje vyraujančių kompleksų sudėties. Izopotencialių tirpalų serijoje ($E_0 = -0,350$ V) nustatyta $R_{\text{CN}} \cong 2$ patvirtino, kad visais atvejais krūvio pernešimo stadijoje tiesiogiai dalyvauja kompleksiniai jonai $\text{Ag}(\text{CN})_2^-$.